Regulation of skeletal myogenesis in C2C12 cells through modulation of Pax7, MyoD, and myogenin via different low-frequency electromagnetic field energies

Jiaqi Bi[a,b,1], Hong Jing[a,1], ChenLiang Zhou[b], Peng Gao[c], Fujun Han[b], Gang Li[d] and
Shiwei Zhang[a,*]
[a]*Harbin Children's Hospital, Harbin, Heilongjiang, China*
[b]*Emergency Department, SongBei Hospital of The Fourth Hospital Affiliated of Harbin Medical
University, Harbin, Heilongjiang, China*
[c]*The First Department of General Surgery, Harbin Children's Hospital, Harbin, Heilongjiang, China*
[d]*The Second Department of Orthopedics, The First Hospital of Yichun, Yichun, Heilongjiang, China*

Abstract.
BACKGROUND: A low-frequency electromagnetic field (LF-EMF) exerts important biological effects on the human body.
OBJECTIVE: We previously studied the immunity and atrophy of gastrocnemius muscles in rats with spinal cord injuries and found that LF-EMF with a magnetic flux density of 1.5 mT exerted excellent therapeutic and preventive effects on reducing myotubes and increasing spatium intermusculare. However, the effects of LF-EMF on all stages of skeletal myogenesis, such as activation, proliferation, differentiation, and fusion of satellite cells to myotubes as stimulated by myogenic *regulatory factors* (MRFs), have not been fully elucidated.
METHODS: This study investigated the optimal LF-EMF magnetic flux density that exerted maximal effects on all stages of C2C12 cell skeletal myogenesis as well as its impact on regulatory MRF*s*.
RESULTS: The results showed that an LF-EMF with a magnetic flux density of 2.0 mT could activate C2C12 cells and upregulate the proliferation-promoting transcription factor PAX7. On the other hand, 1.5 mT EMF could upregulate the expression of MyoD and myogenin.
CONCLUSION: LF-EMF could prevent the disappearance of myotubes, with different magnetic flux densities of LF-EMF exerting independent and positive effects on skeletal myogenesis such as satellite cell activation and proliferation, muscle cell differentiation, and myocyte fusion.

Keywords: C2C12 cells, low-frequency electromagnetic field (LF-EMF), MyoD, myogenin, Pax7

1. Introduction

The human body possesses a natural, stable, but weak current that is able to generate a magnetic field if it is channeled through a non-closed and non-uniform polarization layer as thin and translucent

---

[1]Jiaqi Bi and Hong Jing contributed equally.
*Corresponding author: Shiwei Zhang, Department of General Surgery, Harbin Children's Hospital, Harbin, Heilongjiang
150010, China. E-mail: 356715354@qq.com.

as a muscle fiber [1–3]. The non-uniform polarization layer is formed by a concentration gradient of cations across the cell membrane [4,5]. A low-frequency electromagnetic field (LF-EMF) exerts essential biological effects on the human body, and an LF-EMF within 300 Hz has been demonstrated to stimulate neovascularization, osteogenesis, and nerve regeneration [6–8]. Recently, LF-EMF application has been shown to enhance the recovery of muscle and tendon injuries [9,10].

Physical activity is significantly affected by skeletal muscle atrophy. Besides genetic disorders of muscular atrophy such as Duchenne muscular dystrophy, *skeletal muscle* atrophy can also be classified as disuse atrophy or neurogenic atrophy. Unlike genetic conditions, both these situations may occur on muscle cells that are physiologically normal [11,12]. Patients with disuse atrophy of skeletal muscles can achieve partial rehabilitation with the help of functional exercises, whereas those with neurogenic skeletal muscle atrophy face more challenges during recovery [13,14]. In neurogenic skeletal muscle atrophy, the denervated muscle is prone to aberrant connective tissue proliferation and eventually irreversible atrophy [15]. Recently, a mechanical exoskeleton has been invented as a means to provide ambulatory support to patients with neurological injury [16]. However, the success of this exoskeleton is heavily dependent on non-atrophic skeletal muscles.

Satellite cells are myogenic stem cells and have the potential to differentiate into either new muscle fibers or new nuclei to power existing muscles. Satellite cells appear to be responsive to various types of stimulation such as ultraviolet light, hormones, environmental pressure, friction, and injuries between muscle fibers. These stimulations cause satellite cells to transform into myoblast and muscle cells and finally fusing into functional myotubes [17]. Myogenic regulatory factors (MRFs), especially MyoD and myogenin, are responsible for inducing satellite cell differentiation and are critical in facilitating muscle recovery [18]. MyoD regulation represents a key step in the process of transcribing myoblast-specific genes that ultimately direct satellite cells to differentiate into myoblasts [19]. In contrast, myogenin is mainly involved in the promoter region and is important in modulating myoblast fusion into myotubules. Nevertheless, satellite cells are first activated by regulating the myogenic transcription factor PAX7 [20,21]. This study investigates how LF-EMF affects C2C12 cell skeletal myogenesis. We also explored the optimal magnetic flux density of LF-EMF for each stage of myogenesis to verify the safety and functions of LF-EMF in *in vitro* experiments. Our findings provide a theoretical framework for the clinical application of LF-EMF in translational medicine.

2. Materials and methods

2.1. Low-frequency electromagnetic system

The home-produced solenoid (equipment for LF-EMF production) consists of a 5 mm thick polyvinyl chloride cylinder measuring 24 mm in diameter that is made from 200 turns of 0.9 mm diameter copper wire. The conductive coil is a Helmholtz coil, with LF-EMF production driven by a signal generator and three amplifiers that create a static and alternating current. This device was able to produce a magnetic flux density between 0 mT and 2.5 mT $\pm$ 2% and a 50 Hz frequency. A meter (Model EFA-2; Wandel and Goltermann, Minden, Germany) was used to measure magnetic flux density. Specific data are shown in the reference [22]. The solenoid was placed in an incubator of continuously controlled humidity regulation maintained at 5% CO_2 and 37°C. Measurements were recorded by a lab-view program (control system).

2.2. Cell culture

The C2C12 cell line is a subclone of the C2 mouse myoblast cell line and was procured from the American Type Culture Collection (CRL-1722). Cells were cultured in a high-glucose Dulbecco's

modified Eagle's medium (DMEM; Gibco, USA), supplemented with 10% heat-inactivated fetal bovine serum (FBS; Invitrogen, USA), 1% penicillin/streptomycin solution (Biological Industries, USA), and 4 mM l-glutamine (Biological Industries, USA).

2.3. Cell treatment

Cells were allowed to culture until they were confluent before they were harvested and seeded into flasks at a density of 9.7×10^4 cells/flask. The cells were continuously maintained at 37°C in an atmosphere of 5% CO_2. Experiments investigating the proliferative ability of cells were performed in cells cultured with DMEM supplemented with 10% FBS and 1% penicillin/streptomycin. Experiments examining cell fusion and differentiation instead used cells cultured in DMEM supplemented with 2% horse serum (Invitrogen) and 1% penicillin/streptomycin. Experimental groups involved were the control (CTR) group (0 mT), low-energy (LEN) group (1.5 mT), and high-energy (HEN) group (2.0 mT), with six flasks treated for 12 h/day for 5 days. Sampling and inspection were done daily.

2.4. Cell proliferation

A cell counting method was used to evaluate cell proliferation. Briefly, the culture solution was diluted 10 times and placed onto a blood cell counting plate. The number of cells in the square under a microscope (Leica, Germany) was then quantified to determine the total cell count.

2.5. Immunofluorescent staining and myoblast differentiation into myocytes

Cells were plated on coverslips and cultured using the appropriate cell media. Cells of each stage were cultured for a day in an incubator either with (exposed) or without (control) LF-EMF exposure. Cells were rinsed using PBS and fixed for 15 min in 4% paraformaldehyde. Cell morphology was observed using a phase-contrast microscope (Olympus Company, Japan). Pax7, MyoD, and myogenin levels were evaluated using direct fluorescence by first incubating the cells with anti-Pax7, anti-MyoD, and anti-myogenin toxin (Sigma, USA) for an hour in PBS buffer. Cells were then rinsed three times with PBS before the Hoechst 33342 stain was used to highlight cell nuclei. A fluorescence microscope (Olympus IX51; RT Slider SPOT Diagnostic Instruments, Japan) was then used to observe cell fluorescence. The MyoG-positive cells rate was determined by dividing the number of MyoG-positive cells by the total number of myocytes. The rate of MyoG-positive cells was calculated by averaging the results obtained from five separate images using the ImageJ software.

2.6. RNA extraction and real-time quantitative polymerase chain reaction

Cells in various stages of proliferation, differentiation, and fusion were collected on the first, second, third, fourth, and fifth days, respectively, and homogenized on ice in 1 mL of Trizol reagent. Cell supernatant was obtained by centrifugation at 12,000 rpm for 10 min. Subsequently, 250 μL of chloroform was inserted, and samples were re-centrifuged before adding 0.8 volumes of isopropanol. The supernatant was incubated for 15 min at −20°C and centrifuged again. Precipitates were washed with 75% ethanol before adding DEPC water to dissolve RNA residue. Reverse transcription and RNA detection were carried out in compliance with protocols stipulated by the manufacturer (Servicebio Technology Co., Ltd., Wuhan, China). The primers and reaction conditions are shown in Table 1.

Table 1
Specific primers for real-time polymerase chain reaction analysis

Primer	Sequence
Pax7	5'-CTCAGTGAGTTCGATTAGCCG-3'
	3'- CGCTGTTTCCCTTGGCAGA-5'
MyoD	5'-CGGGACATAGACTTGACAGGC-3'
	3'-AGATACTACTGGGCACAAAGCT-5'
Myogenin	5'-GAGACATCCCCCTATTTCTACCA-3'
	3'-GCTCAGTCCGCTCATAGCC-5'
GAPDH	5'-AAACCRGCCAAGTATGATGA-3'
	3'- TCATTCTTTGGGACCTGGTG-5'

2.7. Western blotting

Pax7, MyoD, and myogenin protein expressions (Sigma, USA) were evaluated by Western blotting. A cell lysis buffer that included protease inhibitors was used to homogenize the cells for 20 min on ice. Samples were then centrifuged for 15 min at $12,000 \times$ g before the supernatant was collected for quantification of protein concentration using a bicinchoninic acid assay protein quantification kit (Abcam, USA). Protein samples were diluted to achieve a standard uniform concentration with a protein extraction reagent. Protein samples were exposed to loading buffer at a ratio of 1:4 v/v before the sample was boiled for 15 min. Equal amounts of protein samples (10 μg) were separated using sodium dodecyl sulfate – polyacrylamide gel electrophoresis (8%–12% acrylamide gels) before being transferred onto a polyvinylidene difluoride membrane (Millipore, Waltham, MA, USA). 5% non-fat milk in Tween 20 (TBST) solution and tris-buffered saline was used to block membranes for 2 h at room temperature. Membranes were then incubated with primary antibodies at 4°C. TBST was used to rinse the membranes three times before secondary antibodies were added. The mixture was allowed to incubate for another 2 h at room temperature. Protein bands were imaged using enhanced chemiluminescence (CW Biotech, Beijing, China) and assessed with densitometry using the Image Quant TL software (GE Healthcare, Uppsala, Sweden).

2.8. Statistical analysis

All statistical analyses were performed using SPSS26.0. Data are depicted in terms of mean $\pm$ SD. Variances between groups were evaluated using the one-way analysis of variance. The S-N-K method was used for multiple comparisons when the variances were uniform, and the Kruskal-Wallis H test was used when the variances were uneven. Statistical significance was granted to P values of < 0.05.

3. Results

3.1. LF-EMF promotes satellite cell proliferation and the upturn fusion of myocytes

In contrast to the LEN group, the HEN group augmented satellite cell proliferation on the first ($P <$ 0.05) and second days ($P < 0.01$), but proliferation subsequently declined thereafter ($P < 0.001$) (Fig. 1A). Likewise, the rate of MyoG-positive cells was enhanced in the HEN group in contrast to the CTR group from the second day ($P < 0.01$, $P < 0.001$), while the LEN group demonstrated augmented the rate of MyoG-positive cells compared to the other two groups throughout the experiment ($P < 0.01$, $P < 0.001$) (Fig. 1B). Our findings demonstrate that low- and high-energy LF-EMFs promoted the proliferation of satellite cells, whereas the low-energy LF-EMF was more effective in promoting the late differentiation of myocytes.
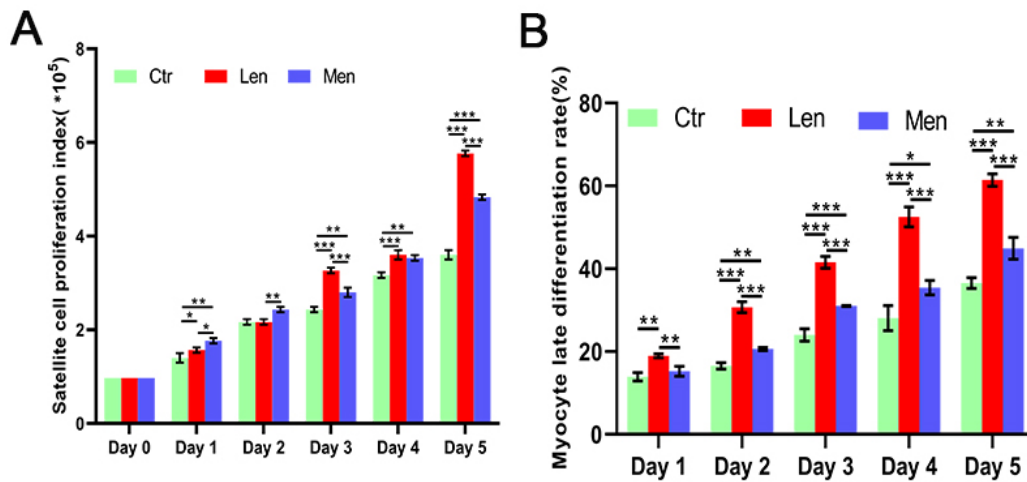
Fig. 1. Effect of LF-EMF on C2C12 cell proliferation (A) and the MyoG-positive cells rate (B) *: $P < 0.05$, **: $P < 0.01$, ***: $P < 0.001$.

3.2. High-energy LF-EMF activates satellite cells

Low-energy LF-EMF increased the concentration of PAX7 only on the first and third days of LF-EMF therapy ($P < 0.05$, $P < 0.01$). There were no significant differences at any other time seen between the LEN and CTR groups. Likewise, the HEN and LEN groups did not differ significantly in terms of PAX7 expression on the third and fourth days ($P = 0.442$, $P = 0.063$). In contrast, high-energy LF-EMF upregulated PAX7 compared to the CTR group throughout the duration of the experiment ($P < 0.05$, $P < 0.01$, $P < 0.001$) (Fig. 2A). Immunofluorescence staining images revealed that the number of blue nuclei in the LEN group was similar to that of the CTR group from the fourth day, while the HEN group had significantly more blue nuclei than the other two groups from the second day. In contrast, PAX7 protein expression (green fluorescence) was higher on the first and fifth days in the LEN group than in the CTR group, with higher PAX7 protein expression in the HEN group throughout the experiment (Fig. 2B). These findings suggest that LF-EMF could upregulate *in vitro* PAX7 mRNA levels and that the high-energy LF-EMF was more effective than low-energy LF-EMF.

3.3. Low-energy LF-EMF promotes the differentiation of myoblasts

Muscle *differentiation* was *induced* by *DMEM*/F-12 supplemented with 2% (v/v) horse serum. In contrast to the CTR group, the level of MyoD in the HEN group on the first and second days was significantly raised ($P < 0.05$, $P < 0.01$). MyoD was significantly upregulated in the LEN group compared with the other two groups throughout the experiment ($P < 0.05$, $P < 0.01$, $P < 0.001$) (Fig. 3A). Immunofluorescence staining showed that C2C12 cells changed into spindle-shaped myoblasts. The CTR group demonstrated a gradual increase in the number of nuclei, with the LEN group having significantly more nuclei than the other two groups. Levels of the MyoD protein increased slowly in the CTR group, with significantly more MyoD protein in the LEN group than in the HEN group (Fig. 3B). These findings demonstrate that low-energy LF-EMF was better at stimulating myoblast differentiation into myocytes.
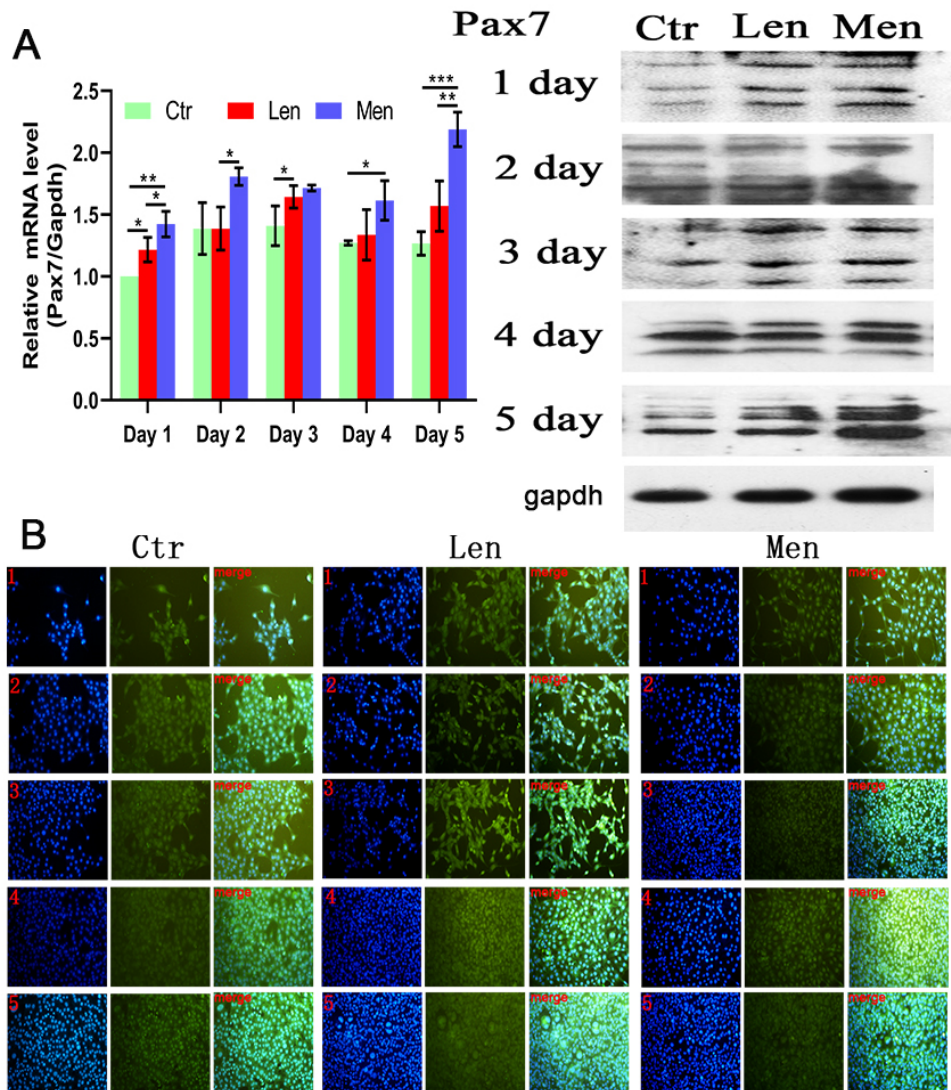
Fig. 2. (A) Level of PAX7 mRNA in C2C12 cells with Western blotting and (B) immunofluorescence staining images showing the activation and proliferation of C2C12 cells over 5 days. *: $P < 0.05$, **: $P < 0.01$, ***: $P < 0.001$.

3.4. Low-energy LF-EMF promotes the late differentiation

The late differentiation of myocytes was *induced* by *DMEM*/F-12 supplemented with 2% (v/v) horse serum. Myogenin expression did not significantly differ between CTR and HEN groups, but there was a significantly higher expression in the LEN group throughout the experiment ($P < 0.01$, $P < 0.001$) (Fig. 4A). Moreover, the number of nuclei in the CTR group significantly increased in differentiated myoblasts. CTR and HEN groups did not demonstrate any variability in terms of myogenin protein expression, in contrast to the LEN group, which did express higher levels of the myogenin protein from the second day compared to the other two groups (Fig. 4B). These results indicated that LF-EMF induced late differentiation of myocyte, especially in the LEN group.
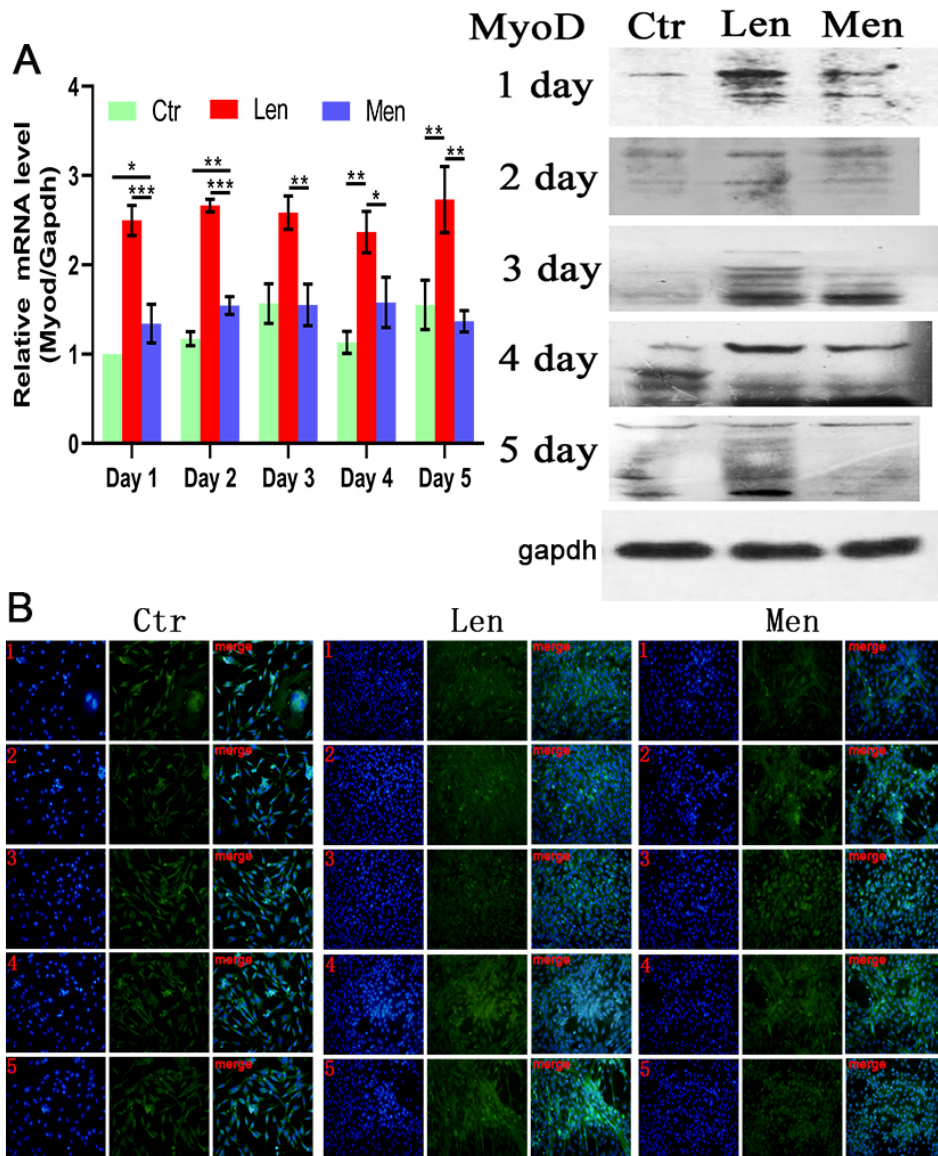
Fig. 3. (A) Level of MyoD mRNA in myoblasts and Western blotting and (B) immunofluorescence staining images showing the differentiation of myoblasts over 5 days. *: $P < 0.05$, **: $P < 0.01$, ***: $P < 0.001$.

4. Discussion

LF-EMF-based therapies have a wide range of medical applications and have been used in delayed union of fractures, stress fractures, bone nonunion, tendon and ligament repair, pain and edema of soft tissues, ulcer healing, protection of cerebral ischemia, and osteoporosis [8–10,23–26]. LF-EMF is non-invasive, more penetrable, less affected by the transmission medium, and reaches target sites easier [27]. Recovery of muscle injuries, as well as muscle maintenance and growth, depending on skeletal myogenesis. This complex biological phenomenon involves myoblast development, differentiation, fusion into primary and
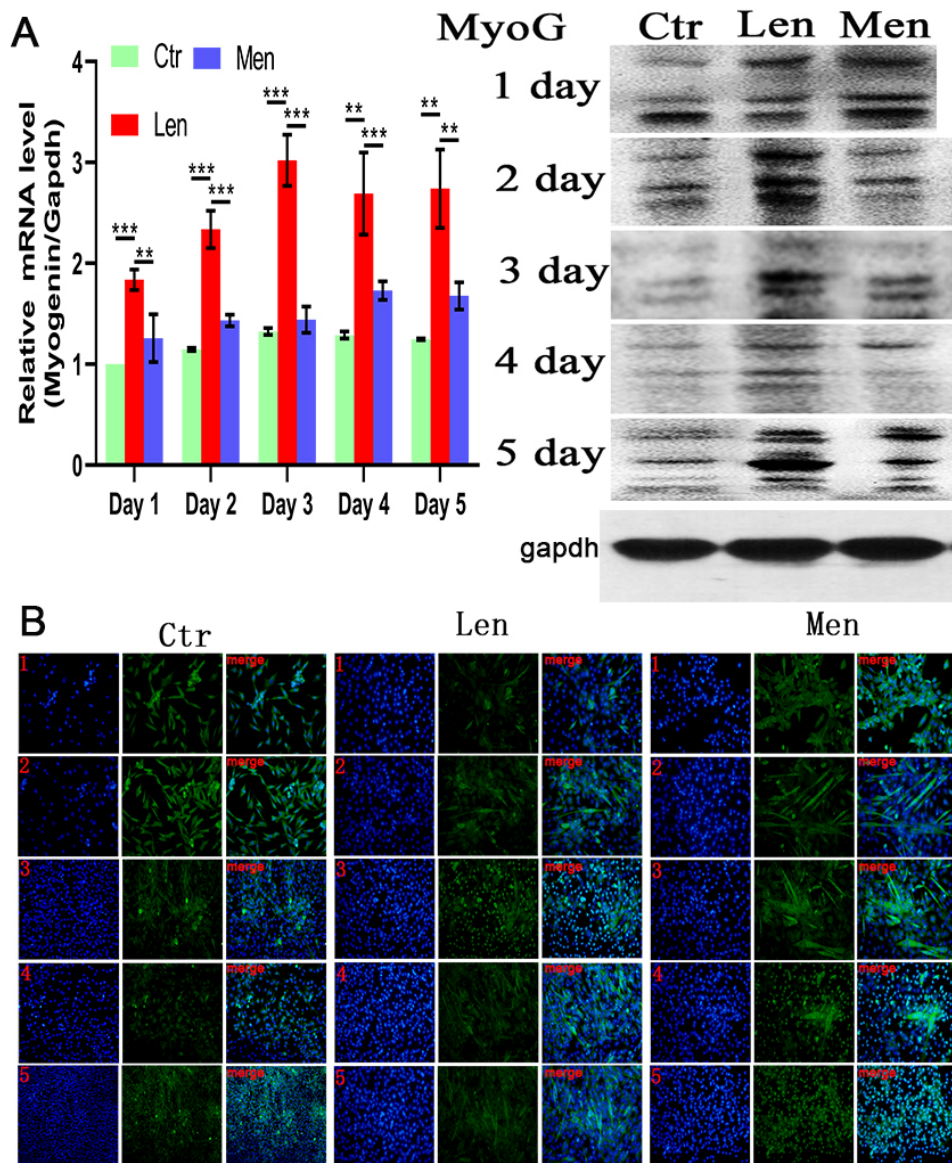
Fig. 4. (A) Level of Myogenin mRNA in muscle cells and Western blotting and (B) immunofluorescence staining images showing the MyoG-positive cells over 5 days. **: $P < 0.01$, ***: $P < 0.001$.

secondary myotubes, and finally maturation into fully developed adult muscle fibers [28]. Skeletal muscles of adult mammals are extremely stable, with minor damage caused by daily wear and tear, maintaining the slow metabolism of muscle fibers, ensuring that they retain their ability of rapid regeneration in severe muscle injury. In-depth studies have identified several transcription factors and MRFs associated with muscle regeneration and repair after injuries and diseases. Among these include PAX7, MRFs, heat shock protein, and the MAPK signaling pathways [29–33]. Several studies outlining the specific roles of these transcription factors and protein kinases in detail in relation to myosatellite cell proliferation, myoblast differentiation, and muscle cell fusion already exist. However, how LF-EMF regulates transcription

factors during the entire process of skeletal muscle regeneration, as well as the optimal energy for each stage of skeletal muscle development from myosatellite cells to myotubes, have yet to be identified.

Skeletal muscle regeneration is similar to embryonic muscle development. The most critical part of this process is the activation and proliferation of satellite cells [34]. Studies have found that continuous activation depletes satellite cells and stagnates skeletal muscle recovery [35,36]. LF-EMF has been proven to exert a proliferation-promoting effect on human umbilical vein endothelial cells, mouse bone cells, endothelial progenitor cells, human epidermal stem cells, and vascular smooth muscle cells [37]. In efforts to deepen the understanding of the role of LF-EMF in muscle repair, we found that high-energy LF-EMF promoted muscle cell proliferation better in the early stage of the experiment, especially on the first and second days, indicating that the LF-EMF had an effect on myoblast cell proliferation. These findings mirrored those of Acharya et al., who found that ELF-EMF stimulation enhanced cellular proliferation [19].

The transcription factor PAX7 is considered to be the most important factor for activating and proliferating satellite cells [38]. Interestingly, we found that low-energy LF-EMF increased the concentration of PAX7 only on the first and third days of LF-EMF therapy ($P < 0.05$, $P < 0.01$), with no significant difference seen between the LEN group and the CTR group at any other time point. The HEN and LEN groups demonstrated no significant difference in terms of PAX7 expression on the third and fourth days. The present study showed that the magnetic flux density of 2.0 mT for an LF-EMF was beneficial in stimulating C2C12 cell proliferation as indicated by the PAX7 upregulation and satellite cell proliferation.

The regeneration of skeletal muscles is a dynamic process that is dominated by satellite cells that are usually present between the sarcolemma and basal lamina of myofibers. Until there is a stimulus for muscle growth or repair, satellite cells are usually mitotically quiescent. Several pathological (such as injury and degenerative diseases) and physiological stimuli (such as exercise) are able to generate a committed population of myoblasts that can either fuse with each other to form new myofibers, repair damaged muscle fibers or fuse with existing myofibers. Myf5 and MyoD are both key players in the development of muscle cells from myosatellite cells. Previous studies on double knockout MyoD-null/Myf5-null mouse revealed the complete absence of skeletal myoblasts. MyoD has also been shown to function as a switch in the differentiation of myoblasts [39,40]. In this study, a lower magnetic flux density of 1.5 mT for an LF-EMF induced the differentiation of myoblasts more effectively than 2.0 mT LF-EMF. Besides, the MyoG exerts significant regulatory functions on primary myotube fusion with secondary multi-nucleated regenerating myotubes. In contrast, compared with the late differentiation-promoting effect of 1.5 mT LF-EMF, an LF-EMF with a magnetic flux density of 2.0 mT had little effect on the late differentiation of muscle cells. This study comprehensively evaluates the effects of different LF-EMF intensities on each stage of skeletal muscle regeneration and development in this study.

5. Conclusion

LF-EMF application was able to modulate satellite cell development into functional muscle fibers, likely through its effect on various transcription factors and MRFs. Moreover, we noted different effects of LF-EMF with different magnetic flux densities. Satellite cell activation and proliferation were triggered with higher energy LE-EMF of 2.0 mT, which was used in this study. However, once the myogenic program was induced, a lower magnetic flux density (1.5 mT) was necessary to trigger myoblast differentiation. Since the myoblasts and muscle cells are both unstable in their respective intermediary states, higher magnetic flux density may cause more cellular stress and heat under the same duration of stimulation. Based on the results of these *in vitro* experiments, we suggest that LF-EMF therapy using different

magnetic flux densities may be more effective than single magnetic flux density in stimulating muscle repair in clinical practice.

Conflict of interest

The authors declare no conflicts of interest.

Data availability

The dat sets used and/or analyzed during the current study are available from the corresponding author on reasonable request.

References

[1] Zuo HY, Liu X, Wang DW, Li Y, Xu XP, Peng RY, Song T. RKIP-Mediated NF-κB Signaling is Involved in ELF-MF-mediated Improvement in AD Rat. International Journal of Medical Sciences. 2018; 15(14): 1658-66.
[2] Tucker JJ, Cirone JM, Morris TR, Nuss CA, Huegel J, Waldorff EI, Zhang NL, Ryaby JT, Soslowsky LJ. Pulsed electromagnetic field therapy improves tendon-to-bone healing in a rat rotator cuff repair model. Journal of Orthopaedic Research. 2017; 35(4): 902-909.
[3] Lim S, Kim SC, Kim JY. Protective Effect of 10-Hz, 1-mT Electromagnetic Field Exposure Against Hypoxia/Reoxygenation Injury in HK-2 Cells. Biomedical and Environmental Sciences. 2015; 28(3): 231-34.
[4] Adler D, Fixler D, Scheinowitz M, Shainberg A, Katz A. Weak electromagnetic fields alter Ca2+ handling and protect against hypoxia-mediated damage in primary newborn rat myotube cultures. Pflügers Archiv – European Journal of Physiology. 2016; 468(8): 1459-65.
[5] Signore S, Sorrentino A, Borghetti G, Cannata A, Meo M, Zhou Y, Kannappan R, Pasqualini F, O'Malley H, Sundman M, Tsigkas N, Zhang E, Arranto C, Mangiaracina C, Isobe K, Sena BF, Kim J, Goichberg P, Nahrendorf M, Isom LL, Leri A, Anversa P, Rota M. Late Na+ current and protracted electrical recovery are critical determinants of the aging myopathy. Nature Communications. 2015; 6(1).
[6] Bodewein L, Schmiedchen K, Dechent D, Stunder D, Graefrath D, Winter L, Kraus T, Driessen S. Systematic review on the biological effects of electric, magnetic and electromagnetic fields in the intermediate frequency range (300 Hz to 1 MHz). Environmental Research. 2019; 171: 247-59.
[7] Martynyuk V, Melnyk M, Artemenko A. Comparison of biological effects of electromagnetic fields with pulse frequencies of 8 and 50 Hz on gastric smooth muscles. Electromagnetic Biology and Medicine. 2016; 35(2): 143-51.
[8] Li RL, Huang JJ, Shi YQ, Hu A, Lu ZY, Weng L, Wang SQ, Han YP, Zhang L, Hao CN, Duan JL. Pulsed electromagnetic field improves postnatal neovascularization in response to hindlimb ischemia. American Journal of Translational Research. 2015; 7(3): 430-44.
[9] Pesqueira T, Costa-Almeida R, Gomes ME. Magnetotherapy: The quest for tendon regeneration. Journal of Cellular Physiology. 2018; 233(10): 6395-405.
[10] Liu MY, Lee CL, Laron D, Zhang NL, Waldorff EI, Ryaby JT, Feeley B, Liu XH. Role of pulsed electromagnetic fields (PEMF) on tenocytes and myoblasts-potential application for treating rotator cuff tears. Journal of Orthopaedic Research. 2017; 35(5): 956-64.
[11] Chiappalupi S, Luca G, Mancuso F, Madaro L, Fallarino F, Nicoletti C, Calvitti M, Arato I, Falabella G, Salvadori L, Di Meo A, Bufalari A, Giovagnoli S, Calafiore R, Donato R, Sorci G. Intraperitoneal injection of microencapsulated sertoli cells restores muscle morphology and performance in dystrophic mice. Biomaterials. 2016; 75: 313-26.
[12] Farini A, Sitzia C, Cassani B, Cassinelli L, Rigoni R, Colleoni F, Fusco N, Gatti S, Bella P, Villa C, Napolitano F, Maiavacca R, Bosari S, Villa A, Torrente Y. Therapeutic potential of immunoproteasome inhibition in duchenne muscular dystrophy. Molecular Therapy. 2016; 24(11): 1898-912.
[13] Moon Y, Balke JE, Madorma D, Siegel MP, Knowels G, Brouckaert P, Buys ES, Marcinek DJ, Percival JM. Nitric oxide regulates skeletal muscle fatigue, fiber type, microtubule organization, and mitochondrial ATP synthesis efficiency through cGMP-Dependent Mechanisms. Antioxidants & Redox Signaling. 2017; 26(17): 966-85.

[14] Fisher AG, Seaborne RA, Hughes TM, Gutteridge A, Stewart C, Coulson JM, Sharples AP, Jarvis JC. Transcriptomic and epigenetic regulation of disuse atrophy and the return to activity in skeletal muscle. The Faseb Journal. 2017; 31(12): 5268-82.

[15] Xu ZR, Feng X, Dong J, Wang ZM, Lee JY, Furdui C, Files DC, Beavers KM, Kritchevsky S, Milligan C, Jin JP, Delbono O, Zhang T. Cardiac Troponin T and fast skeletal muscle denervation in ageing. Journal of Cachexia, Sarcopenia and Muscle. 2017; 8(5): 808-23.

[16] Angeli CA, Boakye M, Morton RA, Vogt J, Benton K, Chen YS, Ferreira CK, Harkema SJ. Recovery of over-ground walking after chronic motor complete spinal cord injury. New England Journal of Medicine. 2018; 379(13): 1244-50.

[17] Knight JD, Kothary R. The myogenic kinome: Protein kinases critical to mammalian skeletal myogenesis. Skeletal Muscle. 2011; 1: 29.

[18] Park GH, Jeong H, Jeong MG, Jang EJ, Bae MA, Lee YL, Kim NJ, Hong JH, Hwang ES. Novel TAZ modulators enhance myogenic differentiation and muscle regeneration. British Journal of Pharmacology. 2014; 171(17): 4051-61.

[19] Acharya S, Peters AM, Norton AS, Murdoch GK, Hill RA. Change in Nox4 Expression is Accompanied by Changes in Myogenic Marker Expression in Differentiating C2C12 Myoblasts. Pflügers Archiv – European Journal of Physiology. 2013; 465(8): 1181-96.

[20] Narasimhan M, Hong J, Atieno N, Muthusamy VR, Davidson CJ, Abu-Rmaileh N, Richardson RS, Gomes AV, Hoidal JR, Rajasekaran NS. Nrf2 deficiency promotes apoptosis and impairs PAX7/MyoD expression in aging skeletal muscle cells. Free Radical Biology and Medicine. 2014; 71: 402-14.

[21] Seale P, Ishibashi J, Scime A, Rudnicki MA. Pax7 is Necessary and Sufficient for the Myogenic Specification of CD45+: Sca1+ Stem Cells from Injured Muscle. Plos Biology. 2004; 2(5): E130.

[22] Liu SN, Bi JQ, Zhang Y, Song QS, Yu M, Sun XW, Qu DF, Liu ST. Preliminary study on the electromagnetic field treatment of osteoporosis in rats. 2020; 47-55.

[23] Gordon T. Electrical stimulation to enhance axon regeneration after peripheral nerve injuries in animal models and humans. Neurotherapeutics. 2016; 13(2): 295-310.

[24] Choi YK, Lee DH, Seo YK, Jung H, Park JK, Cho H. Stimulation of neural differentiation in human bone marrow mesenchymal stem cells by extremely low-frequency electromagnetic fields incorporated with MNPs. Applied biochemistry and Biotechnology. 2014; 174(4): 1233-45.

[25] Huang CY, Chang CW, Chen CR, Chuang CY, Chiang CS, Shu WY, Fan TC, Hsu IC. Extremely low-frequency electromagnetic fields Cause G1 phase arrest through the activation of the ATM-Chk2-p21 Pathway. Plos One. 2014; 9(8): e104732.

[26] Wang L, Saalmann YB, Pinsk MA, Arcaro MJ, Kastner S. Electrophysiological low-frequency coherence and cross-frequency coupling contribute to BOLD Connectivity. Neuron. 2012; 76(5): 1010-20.

[27] Geng DY, Hu G, Wang L, Jia N, Wang FX. Mechanism underlying the bio-effects of an electromagnetic field based on the huang-ferrell model. Genet Mol Res. 2016; 15(2).

[28] McGorm H, Roberts LA, Coombes JS, Peake JM. Turning up the heat: An evaluation of the evidence for heating to promote exercise recovery, muscle rehabilitation and adaptation. Sports Medicine. 2018; 48(6): 1311-28.

[29] Kjøbsted R, Hingst JR, Fentz J, Foretz M, Sanz MN, Pehmøller C, Shum M, Marette A, Mounier R, Treebak JT, Wojtaszewski JFP, Viollet B, Lantier L. AMPK in skeletal muscle function and metabolism. The Faseb Journal. 2018; 32(4): 1741-77.

[30] Chen ZL, Zhang XW, Liu YZ, Liu ZK. Morphine postconditioning protects against reperfusion injury via inhibiting JNK/p38 MAPK and mitochondrial permeability transition pores signaling pathways. Cellular Physiology and Biochemistry. 2016; 39(1): 61-70.

[31] Yokoyama S, Ohno Y, Egawa T, Yasuhara K, Nakai A, Sugiura T, Ohira Y, Yoshioka T, Okita M, Origuchi T, Goto K. Heat shock transcription Factor 1-associated expression of slow myosin heavy chain in mouse soleus muscle in response to unloading with or without reloading. Acta Physiologica. 2016; 217(4): 325-37.

[32] Rahman MM, Ghosh M, Subramani J, Fong GH, Carlson ME, Shapiro LH. CD13 Regulates anchorage and differentiation of the skeletal muscle satellite stem cell population in ischemic injury. Stem Cells. 2014; 32(6): 1564-77.

[33] Zammit PS. Function of the myogenic regulatory factors Myf5, MyoD, Myogenin and MRF4 in Skeletal Muscle. Satellite Cells and Regenerative Myogenesis. 2017; 19-32.

[34] Liu NK, Byers JS, Lam T, Lu QB, Sengelaub DR, Xu XM. Inhibition of cytosolic Phospholipase A2 has neuroprotective effects on motoneuron and muscle atrophy after spinal cord injury. Journal of Neurotrauma. 2021; 38(9): 1327-37.

[35] Hernández-Hernández O, Ávila-Avilés RD, Hernández-Hernández JM. Chromatin landscape during skeletal muscle differentiation. 2020; 578712.

[36] Hernández-Hernández JM, García-González EG, Brun CE, Rudnicki MA. The myogenic regulatory factors, determinants of muscle development. Cell Identity and Regeneration. 2017; 10-18.

[37] Maire P, Santos MD, Madani R, Sakakibara I, Viaut C, Wurmser M. Myogenesis control by SIX transcriptional complexes. 2020; 51-64.

[38]   Fang J, Sia J, Soto J, Wang PP, Li LK, Hsueh YY, Sun R, Faull KF, Tidball JG, Li S. Skeletal Muscle regeneration via the chemical induction and expansion of myogenic stem cells in situ or in vitro. 2021; 864-79.

[39]   Wardle FC. Master control: Transcriptional regulation of mammalian myod. 2019; 211-26.

[40]   Asfour HA, Allouh MZ, Said RS. Myogenic regulatory factors: The orchestrators of myogenesis after 30 years of discovery. 2018; 118-28.